Synthesis, Structures, Solution Behavior, and Reactions of Thiolato-Bridged Diruthenium Carbonyl Phosphine Complexes

Kom-Bei Shiu*

Department of Chemistry, National Cheng Kung University, Tainan, Taiwan 701

Sue-Lein Wang and Fen-Ling Liao

Department of Chemistry, National Tsing Hua University, Hsinchu, Taiwan 300

Michael Y. Chiang

Department of Chemistry, National Sun Yat-Sen University, Kaohsiung, Taiwan 804

Shie-Ming Peng and Gene-Hsiang Lee

Department of Chemistry, National Taiwan University, Taipei, Taiwan 106

Ju-Chun Wang and Lin-Shu Liou

Department of Chemistry, Soochow University, Taipei, Taiwan 111

Received November 13, 1997

Dinuclear thiolato-bridged complexes $[Ru_2(CO)_4(\mu\text{-}SR)_2(PR'_3)_2]$ (R′ = Ph, Me) have been readily prepared from the reaction of $[Ru_2(CO)_4(MeCN)_4(PR'_3)_2][BF_4]_2$ (R′ = Ph (**1**), Me (**2**)) with RSH (R = ^{t}Bu, ^{i}Pr, Ph) and Et_3N at ambient temperature. Although only the syn form of $[Ru_2(CO)_4(\mu\text{-}S^tBu)_2(PPh_3)_2]$ (**3**) and only the anti form of $[Ru_2(CO)_4(\mu\text{-}SPh)_2(PMe_3)_2]$ (**6**) were found, an equilibrium mixture of both the syn (isomer **A**) and anti (isomer **B**) forms was present in solution for $[Ru_2(CO)_4(\mu\text{-}S^iPr)_2(PPh_3)_2]$ (**4**) and $[Ru_2(CO)_4(\mu\text{-}SPh)_2(PPh_3)_2]$ (**5**). The spectral data support that the syn form (**4A**) is the major isomer of **4**, while the anti form (**5B**) is the major isomer of **5**. The two thiolato bridges are located cis to the two phosphine ligands in solid-state structures **3**, **4A**, and **5B**, but they are located cis to only one of the two ligands whereas they are trans to the other in structure **6**. Iodination of **3**−**6** gave one identical product $[Ru_2(CO)_4(\mu\text{-}SR)_2I_2(PR'_3)_2]$ (R′ = Ph, R = ^{t}Bu (**7**), ^{i}Pr (**8**), Ph (**9**); R′ = Me, R = Ph (**10**)). Both spectral and structural evidence shows that **7**−**10** exist in the syn form with no Ru−Ru bonding interaction. The relative orientation of the two thiolato bridges with respect to the two phosphine ligands present in **6** remains in structure **10**, in spite of the change from anti to syn. The reactions of the diiodide complexes $[Ru_2(CO)_4(\mu\text{-}SR)_2I_2(PR'_3)_2]$ with R″S anions give either $[Ru_2(CO)_4(\mu\text{-}SR)_2(PR'_3)_2]$ and R″SSR″ or $[Ru_2(CO)_4(\mu\text{-}SR)_2(SR'')_2(PR'_3)_2]$.

Introduction

Transition-metal complexes with sulfur ligands are of significant interest not only because they often display unusual structures and novel reactivity[1] but also because they can serve as synthetic analogues for the active sites of metalloprotein,[2] and show some relevance to metal sulfide hydrodesulfurization and demercuration catalysts.[3]

Diiron thiolato-bridged complexes, $[Fe_2(CO)_4(\mu\text{-}SR)_2L_2]$ (L = CO, phosphine, phosphite, one or one-half diphosphine or -arsine ligand; R = alkyl, phenyl, or aryl), have been studied extensively in terms of synthesis, reactivity, and spectroscopic measurements.[4] The existence of two isomers, syn and anti, with a common[4−6] arrangement for the two axially coordinated ligands L = phosphine, trans to the metal−metal bond (Chart 1),

* To whom correspondence should be addressed. Fax: (+886) 6 274 0552. E-mail: kbshiu@mail.ncku.edu.tw.

(1) For recent reviews, see: (a) Holm, R. H.; Ciurli, S.; Weigel, J. A. *Prog. Inorg. Chem.* **1990**, *38*, 1. (b) Krebs, B.; Henkel, G. *Angew. Chem., Int. Ed. Engl.* **1991**, *30*, 769. (c) Shibahara, T. *Coord. Chem. Rev.* **1993**, *123*, 73. (d) Saito, T. In *Early Transition Metal Clusters with π-Donor Ligands*; Chisholm, M. H., Ed.; VCH: New York, 1995; Chapter 3. (e) Dance, I.; Fisher, K. *Prog. Inorg. Chem.* **1994**, *41*, 637. (f) Stiefel, E. I. Ed. *Transition Metal Sulfur Chemistry*; American Chemical Society: Washington, DC, 1996.

(2) (a) Coucouvanis, D. *Adv. Inorg. Chem.* **1992**, *38*. 1. (b) Coucouvanis, D. In *Molybenum Enzymes, Cofactors, and Model systems*; Stiefel, E. I., Coucouvanis, D., Newton, W. E., Eds.; American Chemical Society: Washington, DC, 1993; p 304. (c) Rees, D. C.; Chan, M. K.; Kim, J. *Adv. Inorg. Chem.* **1994**, *40*, 89.

(3) (a) Angelici, R. J. *Acc. Chem. Res.* **1988**, *21*, 387. (b) Chen, J.; Daniels, L. M.; Angelici, R. J. *J. Am. Chem. Soc.* **1990**, *112*, 199. (c) Wiegand, B. C.; Friend, C. M. *Chem. Rev.* **1992**, 92, 491. (d) Riaz, V.; Curnow, O. J.; Curtis, M. D. *J. Am. Chem. Soc.* **1994**, *116*, 4357. (e) Bianchini, C.; Meli, A. *J. Chem. Soc., Dalton Trans.* **1996**, 801. (f) Hill, A. F.; Wilton-Ely, J. D. E. T. *Organometallics* **1997**, *16*, 4517.

S0276-7333(97)01002-9 CCC: $15.00
Publication on Web 03/31/1998

Chart 1

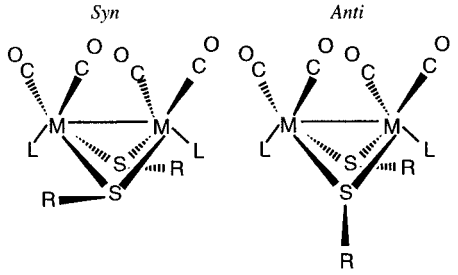

and equilibrated isomerization favoring one isomer or the other were recognized for some types of compounds. Thermal oxidative and reductive decompositions yielding sulfides, disulfides, and thiols were also reported. In contrast the chemistry of diruthenium thiolato-bridged complexes are still relatively unexplored.[5]

In this paper, we present the following new information: (1) the reactions between $[Ru_2(CO)_4(MeCN)_4(PR'_3)_2][BF_4]_2$ (R′ = Ph (**1**), Me (**2**)) and two thiolate anions via RSH/Et_3N can occur even at ambient temperature to afford the Ru−Ru singly bonded compounds $[Ru_2(CO)_4(\mu\text{-}SR)_2(PR'_3)_2]$ (**3**−**6**) (R = ^{t}Bu, ^{i}Pr, Ph; R′ = Ph, Me); (2) the facile interconversion between syn and anti forms of $[Ru_2(CO)_4(\mu\text{-}S^iPr)_2(PPh_3)_2]$ (**4**) and $[Ru_2(CO)_4(\mu\text{-}SPh)_2(PPh_3)_2]$ (**5**) is observed at ambient temperature in solution; (3) the first crystallographically characterized syn and anti forms of the diruthenium thiolato-bridged carbonyl phosphine complexes are presented, adopting either a common geometry in **3**−**5**, with the two thiolato bridges cis to the two phosphine groups observed previously in diiron thiolato-bridged complexes,[4i] or an unprecedented geometry, with the two thiolato bridges cis to one but trans to the other phosphine ligand in **6**; (4) iodination of **3**−**6** affords the single diiodide adducts (**7**−**10**) all in the syn form, where the unique geometry observed in **6** is retained in its diiodide adduct **10**; and (5) the reactions of $[Ru_2(CO)_4(\mu\text{-}SR)_2I_2(PR'_3)_2]$ with R″S$^-$ via R″SH/Et_3N produce either the substituted product $[Ru_2(CO)_4(\mu\text{-}SR)_2(SR'')_2(PR'_3)_2]$ or the reductive-deiodination products $[Ru_2(CO)_4(\mu\text{-}SR)_2(PR'_3)_2]$ with apparently external R″S$^-$ being oxidized into R″SSR″.

(4) (a) Dahl, L. F.; Wei, C.-H. *Inorg. Chem.* **1963**, *2*, 328. (b) Hieber, W.; Kaiser, K. *Chem. Ber.* **1969**, *102*, 4043. (c) Crow, J. P.; Cullen, W. R. *Can. J. Chem.* **1971**, *49*, 2948. (d) De Beer, J. A.; Haines, R. J. *J. Chem. Soc. A* **1971**, 3271. (e) Maresca, L.; Greggio, F.; Sbrignadello, G.; Bor, G. *Inorg. Chim. Acta* **1971**, *5*, 667. (f) De Beer, J. A., Haines, R. J. *J. Organomet. Chem.* **1972**, *36*, 297. (g) De Beer, J. A.; Haines, R. J. *J. Organomet. Chem.* **1972**, *37*, 173. (h) Ellgen, P. C.; Gerlach, J. N. *Inorg. Chem.* **1973**, *12*, 2526. (i) Borgne, G. L.; Grandjean, D.; Mathieu, R.; Poilblanc, R. *J. Organomet. Chem.* **1977**, *131*, 429. (j) Nametkin, N. S.; Tyurin, V. D.; Kukina, M. A. *J. Organomet. Chem.* **1978**, *149*, 355. (k) Shriver, D. F.; Whitmire, K. H. In *Comprehensive Organometallic Chemistry*; Wilkinson, G., Stone, F. G. A., Abel, E. W., Eds.; Pergamon: Oxford, England, 1982; Vol. 4, Chapter 31, p 280. (l) Hawker, P. H.; Twigg, M. V. In *Comprehensive Coordination Chemistry*; Wilkinson, G. W., Gillard, R. D., Eds.; Pergamon: Oxford, England, 1987; Vol. 4. Chapter 44.1, p 1238. (m) Whitmire, K. H, In *Comprehensive Organometallic Chemistry II;* Abel, E. W., Stone, F. G. A., Wilkinson, G., Eds.; Pergamon: Oxford, England, 1995; Vol. 7, Chapter 1, p 65.

(5) (a) Andreu, P. L.; Cabeza, J. A.; Riera, V.; Robert, F.; Jeannin, Y. J. *Organomet. Chem.* **1989**, *372*, C15. (b) Shiu, K.-B.; Li, C.-H.; Chan, T.-J.; Peng, S.-M.; Cheng, M.-C.; Wang, S.-L.; Liao, F.-L. *Organometallics* **1995**, *14*, 524. (c) Soler, J.; Ros, J.; Carrasco, M. R.; Ruiz, A.; Alvarez-Larena, A.; Piniella, J. F. *Inorg. Chem.* **1995**, *34*, 6211.

(6) Andreu, P. L.; Cabeza, J. A.; Miguel, D.; Riera, V.; Villa, M. A.; Garcia-Granda, S. *J. Chem. Soc., Dalton Trans.* **1991**, 533.

Experimental Section

All solvents were dried and purified by standard methods (ethers, paraffins, and arenes from potassium with benzophenone as indicator; halocarbons and acetonitrile from CaH_2 and alcohols from the corresponding alkoxide) and were freshly distilled under nitrogen immediately before use. All reactions and manipulations were carried out in standard Schlenk ware, connected to a switchable double manifold providing vacuum and nitrogen. Reagents were used as supplied by Aldrich. ^{1}H and ^{31}P NMR spectra were measured on a Brueker AMC-400 (^{1}H, 400 MHz; ^{31}P, 162 MHz; ^{13}C, 100 MHz) NMR spectrometer. ^{1}H chemical shifts (δ in ppm, J in hertz) are defined as positive downfield relative to internal $MeSi_4$ (TMS) or the deuterated solvent, while ^{31}P chemical shifts are referred to external 85% H_3PO_4. The IR spectra were recorded on a Bio-Rad FTS 175 instrument. The following abbreviations were used: s, strong (IR); m, medium; s, singlet (NMR); d, doublet; h, heptet; m, multiplet. Microanalyses were carried out by the staff of the Microanalytical Service of the Department of Chemistry, National Cheng Kung University.

Synthesis of $[Ru_2(CO)_4(\mu\text{-}SR)_2(PR'_3)_2]$ (R′ = Ph, R = ^{t}Bu (3), ^{i}Pr (4), Ph (5); R′ = Me, R = Ph (6)). To a solution of $[Ru_2(CO)_4(MeCN)_4(PR'_3)_2][BF_4]_2$[5b] (0.26 mmol) dissolved in 20 mL of MeCN were added carefully deaerated HSR (1 mL) and Et_3N (2 mL). The solution was stirred for 2 h at ambient temperature (ca. 28 °C), forming an orange-yellow precipitate for starting compounds with R′ = Ph and solution for the compounds with R′ = Me. The solvent and volatiles were then removed under vacuum. Recrystallization from CH_2Cl_2/MeOH gave pure product.

3: Anal. Calcd for $C_{48}H_{48}O_4P_2Ru_2S_2$: C, 56.68; H, 4.75. Found: C, 56.61; H, 4.75. Yield: 87%. IR (CH_2Cl_2): ν_{CO}, 2001 s, 1965 m, 1931 s cm^{-1}. ^{1}H NMR (25 °C, acetone-d_6, 400 MHz): δ 0.64 (s, 18 H), 7.53 (m, 30 H). ^{31}P{^{1}H} NMR (25 °C, 162 MHz): δ 27.21 (s, 2 P) in acetone-d_6 and 17.78 (s, 2 P) in $CDCl_3$.

4: Anal. Calcd for $C_{46}H_{44}O_4P_2Ru_2S_2$: C, 55.86; H, 4.48. Found: C, 55.68; H, 4.47. Yield: 88%. IR (CH_2Cl_2): ν_{CO}, 2010 s, 2001 s, 1974 m, 1964 m, 1945 s, 1935 s cm^{-1}. ^{1}H NMR (25 °C, $CDCl_3$, 400 MHz): δ 0.32 (d, 12 H, J = 6.6), 2.54 (h, 2 H) for **4A**; and δ 0.31 (d, 6 H, J = 6.2), 1.03 (d, 6 H, J = 6.2), 2.39 (h, 1 H), 2.71 (h, 1 H) for **4B**. ^{31}P{^{1}H} NMR (25 °C, $CDCl_3$, 162 MHz): δ 19.97 (s, 2 P) for **4A**, and δ 26.54 (s, 2 P) for **4B**.

5: Anal. Calcd for $C_{52}H_{40}O_4P_2Ru_2S_2$: C, 59.08; H, 3.81. Found: C, 59.15; H, 3.92. Yield: 84%. IR (CH_2Cl_2): ν_{CO}, 2016 s, 1979 m, 1951 s cm^{-1}. ^{1}H NMR (25 °C, $CDCl_3$, 400 MHz): δ 6.68 (m, 10 H), 7.38 (m, 30 H). ^{31}P{^{1}H} NMR (25 °C, $CDCl_3$, 162 MHz): δ 21.98 (s, 2 P) for **5A**, and 26.15 (s, 2 P) for **5B**.

6: 89% yield. Anal. Calcd for $C_{16}H_{32}O_4P_2Ru_2S_2$: C, 31.16; H, 5.23. Found: C, 31.07; H, 5.22. IR (CH_2Cl_2): ν_{CO}, 2043 s, 1983 s, 1970 sh, 1937 m cm^{-1}. ^{1}H NMR (25 °C, acetone-d_6, 400 MHz): δ 1.84 (d, 9 H, J = 10.1), 1.70 (d, 9 H, J = 10.1), 7.04 (m, 10 H). ^{31}P{^{1}H} NMR (298 or 220 K, acetone-d_6, 162 MHz): δ 6.42 (s, 1 P), 15.17 (s, 1P).

Iodination of 3−6. To a solution of $[Ru_2(CO)_4(\mu\text{-}SR)_2(PR'_3)_2]$ (0.12 mmol) dissolved in 20 mL of CH_2Cl_2 was added dropwise 4 mL (ca. 0.13 mmol) of an I_2 solution prepared by dissolving 0.129 g (0.51 mmol) of I_2 in 15 mL of CH_2Cl_2. The solution was stirred for 10 min at ambient temperature. The product, **7**−**10**, was separated as a major yellow band by thin-layer chromatography (silica gel, CH_2Cl_2:hexane = 1:1), using TLC plates (Kieselguhr 60 F_{254}, E. Merck), and recrystallized from CH_2Cl_2/MeOH.

$[Ru_2(CO)_4(\mu\text{-}S^tBu)_2I_2(PPh_3)_2]$ (7): 77% yield. Anal. Calcd for $C_{48}H_{48}I_2O_4P_2Ru_2S_2$: C, 45.36; H, 3.81. Found: C, 45.21; H, 3.83. ^{1}H NMR (25 °C, acetone-d_6, 400 MHz): δ 0.76 (s, 18 H), 7.73 (m, 30 H). ^{31}P{^{1}H} NMR (300 or 220 K, acetone-d_6, 162 MHz): δ 44.58 (s, 2 P). IR (CH_2Cl_2): ν_{CO}, 2057 s, 2049 s, 2003 s cm^{-1}.

Table 1. Crystal Data

compd	**3**·CH_3OH·$2H_2O$	**4A**	**5B**	**8**	**10**
formula	$C_{49}H_{48}O_7P_2Ru_2S_2$	$C_{46}H_{44}O_4P_2Ru_2S_2$	$C_{52}H_{40}O_4P_2Ru_2S_2$	$C_{22}H_{28}O_4P_2Ru_2S_2$	$C_{22}H_{28}I_2O_4P_2Ru_2S_2$
fw	1077.1	988.9	1057.8	684.67	988.9
color, habit	orange-yellow, chunk	yellow, rhombohedron	orange-yellow, chunk	yellow, prism	orange-yellow, equant
diffractometer used	Siemens SMART-CCD	Siemens P4	Nonius	Rigaku AFC7S	Siemens SMART-CCD
space group	monoclinic, $C2/c$	orthorhombic, $Cmc2_1$	triclinic, $P\bar{1}$	monoclinic, $P2_1/n$	monoclinic, $P2_1/c$
a, Å	48.905(2)	24.522(4)	9.8356(14)	11.673(3)	10.769(2)
b, Å	10.759(2)	11.318(2)	11.168(3)	17.716(4)	24.144(2)
c, Å	19.528(2)	16.037(4)	22.065(5)	13.496(2)	13.097(2)
α, deg	90	90	82.16(3)	90	90
β, deg	97.97(2)	90	78.92(3)	94.59(2)	112.56(2)
γ, deg	90	90	79.640(16)	90	90
V, Å^3	10175(2)	4451.1(14)	2326.8(8)	2782.0(10)	3144.8(8)
Z	8	4	2	4	4
D_{calcd}, g cm^{-3}	1.406	1.455	1.509	1.635	1.982
λ(Mo Kα), Å	0.710 73	0.710 73	0.7107	0.710 69	0.710 73
F(000)	4384	2208	1063	1368	1792
unit cell detn					
no. 2θ range, deg	whole data	25, 14−28	25, 19−34	25, 15−23	whole data
scan type	hemisphere	$\theta-\omega$	$\theta-2\theta$	$\omega-2\theta$	hemisphere
2θ range, deg	4−54	3−50	3−50	6−47	3−52
h,k,l range	±49,±12,±23	14,30,20	±18,±19,26	13,19,±14	±13,±28,±15
μ(Mo Kα), cm^{-1}	7.85	8.84	4.75	13.76	31.83
cryst size, mm	0.48 × 0.40 × 0.35	0.5 × 0.5 × 0.5	0.50 × 0.50 × 0.60	0.25 × 0.30 × 0.33	0.52 × 0.44 × 0.36
temp, K	296	298	298	297	296
no. of measd rflns	42 104	4428	8198	4501	14 136
no. of unique rflns	8449	2098	8173	4269	5446
no. of obst rflns (N_o)	7104 (>3σ)	1660 (>4σ)	6711 (>2σ)	3400 (>3σ)	4754 (>3σ)
R^a, $R_w{}^a$	0.038, 0.043	0.041, 0.050	0.026, 0.030	0.027, 0.034	0.034, 0.042
GOF^a	1.22	1.04	1.64	1.27	1.01
refinement program	SHELXTL-PLUS	SHELXTL-PLUS	NRCVAX	TEXSAN	SHELXTL-PLUS
no. of ref params (N_p)	560	138	560	289	308
weighting scheme	$[\sigma^2(F_o) + 0.0006F_o^2]^{-1}$	$[\sigma^2(F_o) + 0.0010F_o^2]^{-1}$	$[\sigma^2(F_o) + 0.0001F_o^2]^{-1}$	$[\sigma^2(F_o)]^{-1}$	$[\sigma^2(F_o) + 0.0009F_o^2]^{-1}$
second extinct coeff	0	0	$1.91(15) \times 10^{-4}$		
$(\Delta\rho)_{max}$, e Å^{-3}	1.12	0.89	0.0065	0.32	0.97
$(\Delta\rho)_{min}$, e Å^{-3}	−0.65	−0.63	−0.53	−0.56	−0.70

^{a} $R = [\sum||F_o| - |F_c||/\sum|F_o|]$. $R_w = [\sum w(|F_o| - |F_c|)^2/\sum w|F_o|^2]^{1/2}$. GOF $= [\sum w(|F_o| - |F_c|)^2/(N_o - N_p)]^{1/2}$.

$[Ru_2(CO)_4(\mu\text{-}S^iPr)_2I_2(PPh_3)_2]$ (8): 83% yield. Anal. Calcd for $C_{46}H_{44}I_2O_4P_2Ru_2S_2$: C, 44.45; H, 3.57. Found: C, 44.21; H, 3.60. ^{1}H NMR (27 °C, acetone-d_6, 400 MHz): δ 0.95 (d, 12 H, J = 6.7), 2.99 (h, 2 H), 7.60 (m, 30 H). ^{31}P{^{1}H} NMR (300 or 220 K, acetone-d_6, 162 MHz): δ 46.65 (s, 2 P). IR (CH_2Cl_2): ν_{CO}, 2059 s, 2051 s, 2005 s cm^{-1}.

$[Ru_2(CO)_4(\mu\text{-}SPh)_2I_2(PPh_3)_2]$ (9): 85% yield. Anal. Calcd for $C_{52}H_{40}I_2O_4P_2Ru_2S_2$: C, 47.64; H, 3.08. Found: C, 47.43; H, 3.11. ^{1}H NMR (27 °C, acetone-d_6, 400 MHz): δ 7.47 (m, 40 H). ^{31}P{^{1}H} NMR (300 or 220 K, acetone-d_6, 162 MHz): δ 50.97 (s, 2 P). IR (CH_2Cl_2): ν_{CO}, 2070 sh, 2062 s, 2017 s cm^{-1}.

$[Ru_2(CO)_4(\mu\text{-}SPh)_2I_2(PMe_3)_2]$ (10): 82% yield. Anal. Calcd for $C_{22}H_{28}I_2O_4P_2Ru_2S_2$: C, 28.16; H, 3.01. Found: C, 28.11; H, 3.01. ^{1}H NMR (27 °C, acetone-d_6, 400 MHz): δ 1.74 (d, 9 H, J = 10.8), 1.84 (d, 9 H, J = 10.8), 7.53 (m, 10 H). ^{31}P{^{1}H} NMR (300 or 220 K, acetone-d_6, 162 MHz): δ 18.47 (s, 1 P), 27.77 (s, 1 P). IR (CH_2Cl_2): ν_{CO}, 2047 s, 2008 sh, 1991 s, 1960 m cm^{-1}.

Reaction of $[Ru_2(CO)_4(\mu\text{-}SR)_2I_2(PR'_3)_2]$ with R″SH (R″ = ^{t}Bu, ^{i}Pr, Ph) and Et_3N. (a) Reactions between **7** and R″SH/Et_3N and that between **9** and ^{t}BuSH/Et_3N are quite similar, and only one typical example is shown below. Compound **7** (445 mg, 0.35 mmol) was dissolved in 20 mL of MeCN, and to this solution were then added 1 mL of PhSH and 2 mL of Et_3N. The solution was stirred for 2 h, forming a orange-yellow precipitate. The solvent and volatiles were then removed under vacuum, and the residue was taken up in a minimum amount of CH_2Cl_2. The products were separated by thin-layer chromatography using CH_2Cl_2/hexane mixed solvents to give 63 mg of PhSSPh (83%) and 274 mg of **3** (77%). (b) Reaction between **9** and PhSH/Et_3N: Compound **9** (203 mg, 0.155 mmol) was dissolved in 10 mL of MeCN to form a clear yellow solution, and to this solution were then added 1 mL of Et_3N and 0.5 mL of PhSH. Upon addition of PhSH, the orange-yellow color developed immediately and an orange-yellow precipitate appeared within 3 min. The suspension was stirred for an additional 30 min. The precipitate was collected, washed with 5 mL of MeOH three times, and dried under vacuum to afford 148 mg of the product $[Ru_2(CO)_4(\mu\text{-}SPh)_2(SPh)_2(PPh_3)_2]$ (**11**) in 75% yield. Anal. Calcd for $C_{64}H_{50}O_4P_2Ru_2S_4$: C, 60.27; H, 3.95. Found: C, 60.17; H, 3.95. IR (CH_2Cl_2): ν_{CO}, 2045 s, 2032 sh, 1985 s cm^{-1}. ^{1}H NMR (27 °C, $CDCl_3$, 400 MHz): δ 7.39 (m, 50 H). ^{31}P{^{1}H} NMR (300 K, $CDCl_3$, 162 MHz): δ 19.47 (s, 2 P).

Single-Crystal X-ray Diffraction Studies of 3, 4A, 5B, 6, and 10. Suitable single crystals were grown from CH_2Cl_2/MeOH or CH_2Cl_2/hexane at room temperature and chosen for single crystal structure determinations. The X-ray diffraction data of **4A**, **5B**, and **6** were measured on a four-circle diffractometer, and those of **3** and **10** were measured in frames with increasing ω (0.3 deg/frame) and with the scan speed at 10.00 s/frame on a Siemens SMART-CCD instrument, equipped with a normal focus and 3 kW sealed-tube X-ray source. For data collected on the four-circle diffractometer, three standard reflections were monitored every hour or every 50 reflections throughout the collection. The variation was less than 2%. Empirical absorption corrections were carried out based on an azimuthal scan. For **6**, the structure was solved by direct methods and refined by a full-matrix least-squares procedure using TEXSAN.[7] For **5B**, the structures were solved by the heavy-atom method and refined by a full-matrix least-squares procedure using NRCVAX.[8] For **3**, **4A**, and **10**, the structures were solved by direct methods and refined by a full-matrix least-squares procedure using SHELXTL-PLUS.[9] Neutral atom scattering factors for non-hydrogen atoms and the values for $\Delta f'$ and $\Delta f''$ described in each software[7−9] were used. The other essential details of single-crystal data measurement and refinement are listed in Table 1. One molecule of MeOH and two molecules of H_2O were found in the asymmetric unit of

(7) Crystal Structure Analysis Package, Molecular Structure Corporation, Texas, 1985 and 1992.

(8) Gabe, E. J.; Le page, Y.; Charland, J.-P.; Lee, F. L.; White, P. S. *J. Appl. Crystallogr.* **1989**, *22*, 384.

(9) (a) Sheldrick, G. M. *SHELXTL-Plus Crystallographic System*, release 4.21; Siemens Analytical X-ray Instruments: Madison, WI, 1991. (b) Siemens Analytical X-ray Instruments Inc.: Karlsruhe, Germany, 1991.

Scheme 1

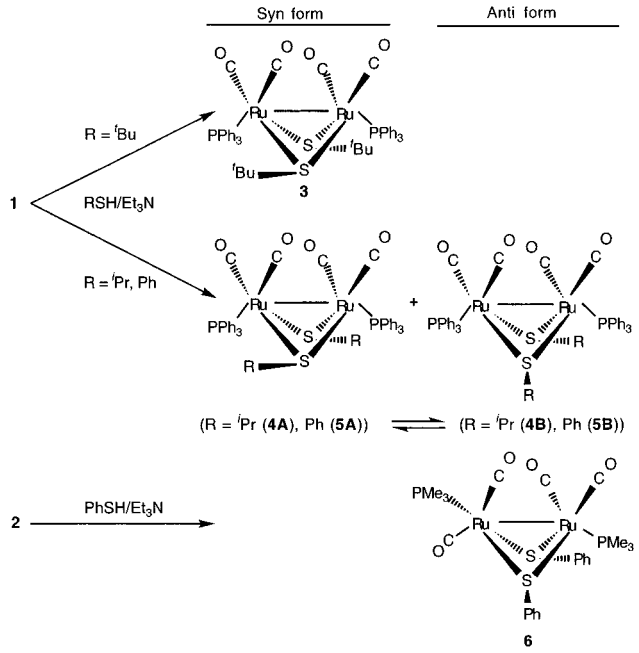

the crystals used for **3**. The solvent hydrogen positions in this structure were not included in the structure refinement.

Results and Discussion

Synthesis, Structures, and Solution Behavior of $[Ru_2(CO)_4(\mu\text{-}SR)_2(PR'_3)_2]$ (3−6). Following one of our recent reports that the acetonitrile ligands of **1** and **2** can be easily replaced by weak anions such as NO_3^-,[10] we rediscovered that the temperature for reaction between **1** and 1,2-benzenedithiol to produce $[Ru_2(CO)_4(\mu,\eta^2\text{-}S_2C_6H_4)(PPh_3)_2]$[5b] can be reduced to the ambient temperature. Likewise the reaction of **1** and **2** with a thiol in the presence of a base such as Et_3N can occur readily at ambient temperature to give **3**−**6** in satisfactory yield (Scheme 1). The diruthenium trimethylphosphine derivative was found to be more air-sensitive than the triphenylphosphine analogue. Both the thiol and Et_3N should be carefully deaerated before addition to compounds **1** and **2**, especially for the preparation of **6**. This compound is orange-yellow. However, when aerated thiol and Et_3N were used to react with **2**, the resulted orange-red to red products contained obviously multiple components displaying more than 15 $^{31}P\{^1H\}$ NMR singlets between δ −20 and 33 in $CDCl_3$.

Compound **3** was previously reported to be formed either from the thermal degradation of $[Ru_3(CO)_9(PPh_3)_3]$ with ^{t}BuSH by Cabeza et al. in 1989[5a] or from a long (20 h) thermal displacement reaction between $[Ru_2(CO)_4(\mu\text{-}O_2CH)_2(PPh_3)_2]$ and the thiol in refluxing toluene (bp 110 °C) by Ros et al. in 1995.[5c] Although it is not unreasonable that both syn and anti isomers are produced under these reaction conditions, the $^{31}P\{^1H\}$ chemical shifts of Ros's two isomers are rather high at δ 45.3 for syn and 39.5 for anti, compared with the values of 23.87 reported for Cabeza's compound[5a] and 17.78 measured for **3** in our laboratory. The $^{31}P\{^1H\}$ singlet observed for this compound remains at 220 K

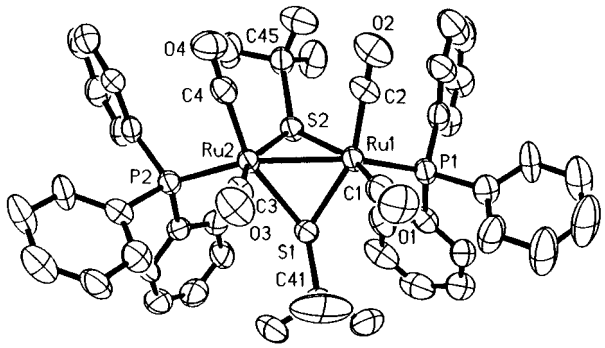

Figure 1. ORTEP plot of $[Ru_2(CO)_4(\mu\text{-}S^tBu)_2(PPh_3)_2]$ (**3**). Selected bond distances (Å): Ru(1)−Ru(2) = 2.640(1), Ru(1)−S(1) = 2.319(1), Ru(1)−S(2) = 2.422(1), Ru(1)−P(1) = 2.449(1), Ru(1)−C(1) = 1.867(4), Ru(1)−C(2) = 1.867(5), Ru(2)−S(1) = 2.564(1), Ru(2)−S(2) = 2.466(1), Ru(2)−P(2) = 2.265(1), Ru(2)−C(3) = 1.887(4), Ru(2)−C(4) = 1.945(5). Selected bond angles (deg): Ru(1)−Ru(2)−S(1) = 52.9(1), Ru(1)−Ru(2)−S(2) = 56.5(1), Ru(1)−Ru(2)−P(2) = 148.6(1), Ru(2)−Ru(1)−S(1) = 61.9(1), Ru(2)−Ru(1)−S(2) = 58.1(1), Ru(2)−Ru(1)−P(1) = 150.3(1), Ru(1)−S(1)−Ru(2) = 65.2(1), Ru(1)−S(2)−Ru(2) = 65.4(1), P(1)−Ru(1)−S(1) = 96.6(1), P(1)−Ru(1)−S(2) = 97.9(1), P(2)−Ru(2)−S(1) = 100.8(1), P(2)−Ru(2)−S(2) = 100.6(1).

in acetone-d_6, or at 420 K in acetophenone-d_3, indicating probably the presence of only one isomer at either high or low temperature. On the basis of the three-carbonyl-stretching-band pattern observed for **3** dissolved in CH_2Cl_2, the structure is not in the anti form (C_s symmetry), but in the syn geometry (C_{2v} symmetry), which was confirmed by X-ray diffraction methods (Figure 1). The high-temperature ^{31}P NMR evidence reflects that the syn geometry is more stable thermodynamically than the anti form, if this form can be prepared in some way. It is hence quite surprising that Ros's isolated "syn" isomer was found to be a minor product with "syn"/"anti" = 1:8.[5c]

The isolated **4** and **5** exist in solution as equilibrium mixtures of syn (isomer **A**) and anti (isomer **B**) isomers, as evidenced by the following: (1) similar NMR and IR spectra were obtained by dissolving either the products **4** and **5** or their single crystals (**4A** and **5B**); (2) the syn:anti ratio was found to be changeless within experimental error, even after a toluene solution of **4** (or **5**) was heated under reflux for more than 80 h; and (3) two exchange cross peaks, indicating clearly $P_{syn} \leftrightarrow P_{anti}$, were shown in the $^{31}P\{^1H\}$ NOESY NMR experiments[11] for **4** and **5** in $CDCl_3$ at 298 K. The spectral data support that **4A** (the syn form) is the major isomer for **4**, whereas **5B** (the anti form) is the major component for **5**. The observed syn/anti (or **4A**:**4B**) integration ratio of 1.16:1 based on the ^1H NMR doublets assigned for the methyl groups of ^{i}Pr of **4** is close to that of 1.14:1 based on the inverse-gated $^{31}P\{^1H\}$ NMR singlets (i.e., without NOE) in $CDCl_3$. Similarly, the calculated integration ratio between one carbonyl ^{13}C NMR singlet for **5A** (the syn form) and two carbonyl singlets for **5B** (the anti form) is 1.14:1:1, based on the observed **5A**:**5B** integration ratio of 1:1.766 found as two inverse-gated $^{31}P\{^1H\}$ NMR singlets, is close to the observed integration ratio of 1.13:1:1 based on the three broad

(10) Shiu, K.-B.; Yang, L.-T.; Jean, S.-W.; Li, C.-H.; Wu, R.-L.; Wang, J.-C.; Liou, L.-S.; Chiang, M. Y. *Inorg. Chem.* **1996**, *35*, 7845.

(11) Bodenhausen, G.; Ernst, R. R. *J. Am. Chem. Soc.* **1982**, *104*, 1304.

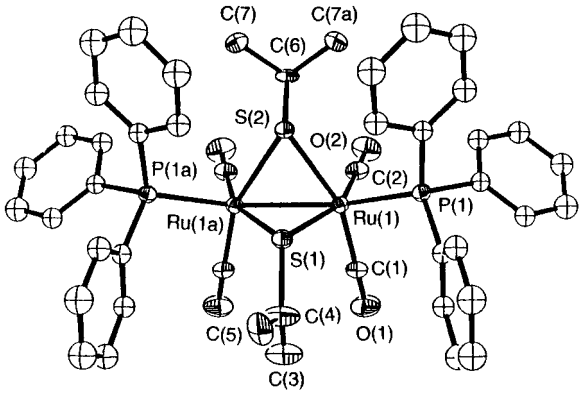

Figure 2. ORTEP plot of $[Ru_2(CO)_4(\mu\text{-}S^iPr)_2(PPh_3)_2]$ (**4A**). Selected bond distances (Å): Ru(1)−Ru(1a) = 2.694(1), Ru(1)−S(1) = 2.424(3), Ru(1)−S(2) = 2.422(3), Ru(1)−P(1) = 2.375(3), Ru(1)−C(1) = 1.874(10), Ru(1)−C(2) = 1.855(10). Selected bond angles (deg): Ru(1a)−Ru(1)−S(1) = 56.3(1), Ru(1a)−Ru(1)−S(2) = 56.2(1), Ru(1a)−Ru(1)−P(1) = 148.7(1), Ru(1)−S(1)−Ru(1a) = 67.5(1), P(1)−Ru(1)−S(1) = 97.5(1), P(1)−Ru(1)−S(2) = 102.6(1).

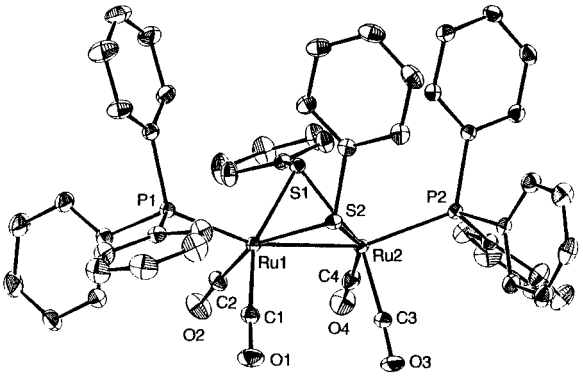

Figure 3. ORTEP plot of $[Ru_2(CO)_4(\mu\text{-}SPh)_2(PPh_3)_2]$ (**5B**). Selected bond distances (Å): Ru(1)−Ru(2) = 2.6788(10), Ru(1)−S(1) = 2.4285(9), Ru(1)−S(2) = 2.4358(11), Ru(1)−P(1) = 2.3897(11), Ru(1)−C(1) = 1.868(3), Ru(1)−C(2) = 1.861(3), Ru(2)−S(1) = 2.4260(8), Ru(2)−S(2) = 2.4323(9), Ru(2)−P(2) = 2.3762(11), Ru(2)−C(3) = 1.874(3), Ru(2)−C(4) = 1.870(3). Selected bond angles (deg): Ru(2)−Ru(1)−S(1) = 51.463(24), Ru(2)−Ru(1)−S(2) = 56.55(3), Ru(2)−Ru(1)−P(1) = 159.917(24), Ru(1)−Ru(2)−S(1) = 56.55(3), Ru(1)−Ru(2)−S(2) = 56.68(3), Ru(1)−Ru(2)−P(2) = 156.929(24), Ru(1)−S(1)−Ru(2) = 66.98(3), Ru(1)−S(2)−Ru(2) = 66.77(3), P(1)−Ru(1)−S(1) = 109.04(4), P(1)−Ru(1)−S(2) = 109.96(4), P(2)−Ru(2)−S(1) = 106.57(4), P(2)−Ru(2)−S(2) = 107.81(4).

^{13}C NMR carbonyl singlets measured in $CDCl_3$. Both the $^{31}P\{^1H\}$ NMR singlet and the ^{13}C NMR carbonyl singlet for the syn form were observed at an upfield position relative to those for the anti form ($^{31}P\{^1H\}$ NMR δ 19.97 for **4A** vs 26.54 for **4B** and 21.98 for **5A** vs. 26.15 for **5B**; $^{13}C\{^1H\}$ NMR 202.0 for **5A** vs 203.4 and 204.6 for **5B**). The single-crystal structures were determined by X-ray diffraction methods, confirming the stereochemistry with the syn form for **4A** (Figure 2) and the anti form for **5B** (Figure 3). Quite coincidentally, the major isomer is the one giving the structures. The spectral and the X-ray crystal structural evidence apparently explain why the two isomers of **4** and **5** cannot be separated in our hands by either silica or alumina column chromatography by CH_2Cl_2/hexane mixtures, although such a separation method was previously reported in obtaining one "syn" and two "anti" isomers of a similar compound, $[Ru_2(CO)_4(\mu\text{-}SBz)_2(PPh_3)_2]$ (Bz = benzyl), by Ros's group.[5c] The syn−anti equilibria of the organothio-bridged deriviatives of iron carbonyl, $[Fe_2(CO)_6(\mu\text{-}SR)_2]$ (with R = Me, Et), and of their monosubstitution products, $[Fe_2(CO)_5(\mu\text{-}SMe)_2(P^n\text{-}Bu_3)]$, were reported previously to have the predominant form in anti geometry for the former but in syn geometry for the latter.[4e] The disubstitution products of a related selenium compound, $[Ru_2(CO)_6(\mu\text{-}SePh)_2]$, with PPh_3 were also found to consist of both forms, with the anti mode favored.[6] Apparently both steric and electronic factors should be combined to account for the different ratio between the two forms.[4g,h]

Dinuclear thiolato-bridged phosphine carbonyl complexes $[M_2(CO)_4(\mu\text{-}SR')_2(PR_3)_2]$ (M = Fe, Ru) were rarely characterized by X-ray diffraction methods and limited in the syn form of $[Fe_2(CO)_4(\mu\text{-}SMe)_2(PMe_3)_2]$ in 1977,[4i] and no crystal structures containing diruthenium analogues have been characterized so far. Hence, **3**, **4A**, and **5B** are the first crystallographically characterized syn and anti structures of diruthenium thiolato-bridged carbonyl phosphine complexes. The Ru−Ru distances of 2.640(1) Å in **3**, 2.694(1) Å in **4A**, and 2.679(1) Å in **5B** are similar to each other and fall within the range 2.558−2.873 Å of other singly Ru−Ru bonded complexes with ligation of PPh_3 ligands.[10,12] Structure **4A** has a crystallographically imposed mirror plane containing the midpoint of the Ru−Ru bond, two sulfur atoms, and four carbon atoms, C(3)−C(6) (Figure 2). Like the previously reported structure with two thiolato bridges, $[Fe_2(CO)_4(\mu\text{-}SMe)_2(PMe_3)_2]$,[4i] and those with one dithiolato bridge, $[Ru_2(CO)_4(\mu,\eta^2\text{-}S_2(C_6H_4)(PPh_3)_2]$[5b] and $[Ru_2(CO)_4(\mu,\eta^2\text{-}S_2(CH_2)_3)(PPh_3)_2]$,[5c] the three thiolato-bridged structures **3** (Figure 1), **4A** (Figure 2), and **5B** (Figure 3) follow to have a common structure type with the two thiolato bridges all being located cis to the two phosphine groups.

Like **4** and **5**, product **6** exhibited two $^{31}P\{^1H\}$ NMR singlets at δ 6.42 and 15.17 at ambient temperature (298 K) and at a low temperature (220 K). However, the single-crystal X-ray structure evidence of **6** did not support the presence of both syn and anti isomers in solution, but revealed an unprecedented structure type for only one anti isomer. The two thiolato bridges are located cis to one but trans to the other phosphine ligand, resulting in two inequivalent phosphine atoms and two $^{31}P\{^1H\}$ NMR singlets in the NMR spectra, with d(Ru−Ru) = 2.6923(8) Å in **6** (Figure 4). The four-band ν_{CO} pattern displayed by a CH_2Cl_2 solution of **6** in an IR spectrum is consistent with the C_1 symmetry of this structure. However, the ν_{CO} pattern should not be overemphasized without consideration of other evidence such as NMR results in the characterization of the related structures, for the bands may be overlapped into a different pattern or may not be resolved by the IR instrument, explaining a six-band and a three-band pattern observed for **4** and **5**, respectively, each containing an equilibrium mixture of two differently weighted

(12) (a) Sherlock, S. J.; Cowie, M.; Singleton, E.; Steyn, M. M. de V. *J. Organomet. Chem.* **1989**, *361*, 353. (b) Garcia-Granda, S.; Obeso-Rosete, R.; Gonzalez, J. M. R.; Anillo, A. *Acta Crystallogr.* **1990**, *C46*, 2043. (c) Shiu, K.-B.; Peng, S.-M.; Cheng, M.-C. *J. Organomet. Chem.* **1993**, *452*, 143. (d) Klemperer, W. G.; Bianxia, Z. *Inorg. Chem.* **1993**, *32*, 5821.

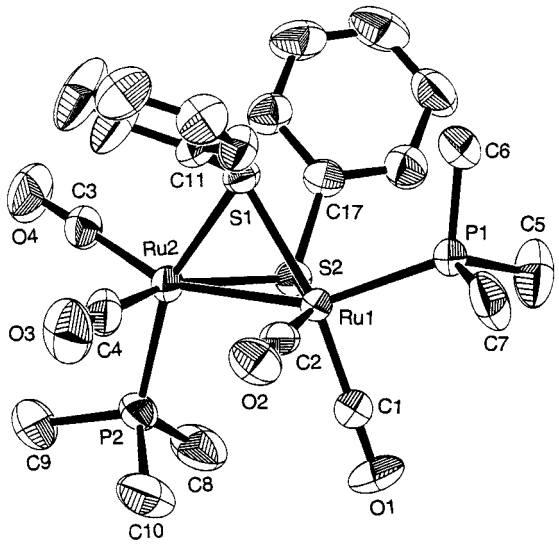

Figure 4. ORTEP plot of $[Ru_2(CO)_4(\mu\text{-SPh})_2(PMe_3)_2]$ (**6**). Selected bond distances: Ru(1)−Ru(2) = 2.6923(8), Ru(1)−S(1) = 2.423(1), Ru(1)−S(2) = 2.433(1), Ru(1)−P(1) = 2.357(1), Ru(1)−C(1) = 1.862(4), Ru(1)−C(2) = 1.868(5), Ru(2)−S(1) = 2.417(1), Ru(2)−S(2) = 2.407(1), Ru(2)−P(2) = 2.327(1), Ru(2)−C(3) = 1.891(4), Ru(2)−C(4) = 1.880(5) Å. Selected bond angles: Ru(2)−Ru(1)−S(1) = 56.09(3), Ru(2)−Ru(1)−S(1) = 55.76(3), Ru(2)−Ru(1)−P(1) = 151.95(3), Ru(1)−Ru(2)−S(1) = 56.32(3), Ru(1)−Ru(2)−S(2) = 56.65(3), Ru(1)−Ru(2)−P(2) = 102.74(3), Ru(1)−S(1)−Ru(2) = 67.60(3), Ru(1)−S(2)−Ru(2) = 67.60(3), P(1)−Ru(1)−S(1) = 99.71(4), P(1)−Ru(1)−S(2) = 109.13(4), P(2)−Ru(2)−S(1) = 159.04(4), P(2)−Ru(2)−S(2) = 90.81(4)°.

Scheme 2

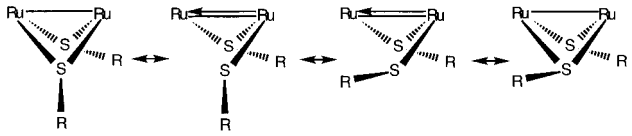

syn and anti isomers. A mechanism probably involving conversion of a bridging into a terminal thiolato group with concomitant formation of multiple Ru−Ru bonding interactions is proposed to account for the equilibrium process between the syn and anti forms of **4** and **5** in solution (Scheme 2).

Synthesis, Structures, and Reactions of $[Ru_2(CO)_4(\mu\text{-SR}')_2I_2(PR_3)_2]$ (7−10). The electrophilic addition of I_2 to CH_2Cl_2 solutions of **3**−**6** generates almost immediately at ambient temperature the diiodide adducts $[Ru_2(CO)_4(\mu\text{-SR}')_2I_2(PR_3)_2]$ (**7**−**10**) (Scheme 3). It appears that there are two different classes of products, as shown in the three-band and the four-band ν_{CO} patterns observed for **7**−**9** and **10**, respectively. Quite coincidentally, the difference between the highest ν_{CO} bands of **7**−**10** and their respective precursor compounds **3**−**6** is as high as about 50 cm^{-1} for **7**−**9** and as low as 4 cm^{-1} for **10** (2057 in **7** vs 2001 in **3**; 2059 in **8** vs 2001 in **4**; 2070 in **9** vs 2016 in **4**; 2047 in **10** vs 2043 cm^{-1} in **6**). The single crystals of **10** were easily grown from CH_2Cl_2/hexane at ambient temperature, and the structure was soon found to keep the unique structure just like the precursor **6** but change the geometry from anti in **6** into syn in **10** (Figure 5). This novel structure with inequivalent phosphine atoms remains not only in the solid state but also in solution, as shown with two observed $^{31}P\{^1H\}$ NMR singlets at δ 18.47 and 27.77 in

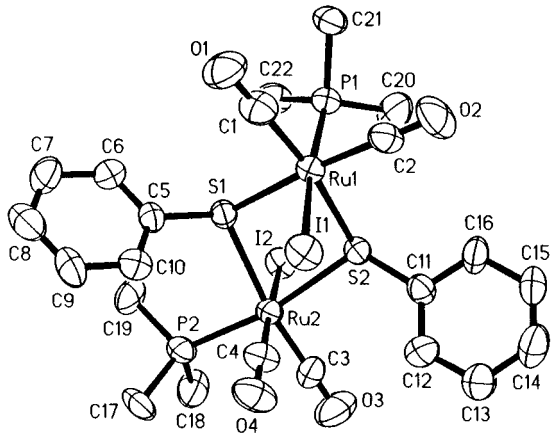

Figure 5. ORTEP plot of $[Ru_2(CO)_4(\mu\text{-SPh})_2I_2(PMe_3)_2]$ (**10**). Selected bond distances (Å): Ru(1)−I(1) = 2.799(1), Ru(1)−S(1) = 2.466(1), Ru(1)−S(2) = 2.458(1), Ru(1)−P(1) = 2.337(1), Ru(1)−C(1) = 1.886(6), Ru(1)−C(2) = 1.869(6), Ru(2)−S(1) = 2.471(1), Ru(2)−S(2) = 2.463(1), Ru(2)−P(2) = 2.360(1), Ru(2)−C(3) = 1.865(9), Ru(2)−C(4) = 1.859(7). Selected bond angles (deg): I(1)−Ru(1)−P(1) = 171.6(1), I(2)−Ru(2)−C(4) = 172.7(2), Ru(1)−S(1)−Ru(2) = 98.6(1), Ru(1)−S(2)−Ru(2) = 99.1(1), P(1)−Ru(1)−S(1) = 91.5(1), P(1)−Ru(1)−S(2) = 90.2(1), P(2)−Ru(2)−S(1) = 94.5(1), P(2)−Ru(2)−S(2) = 168.3(1).

Scheme 3

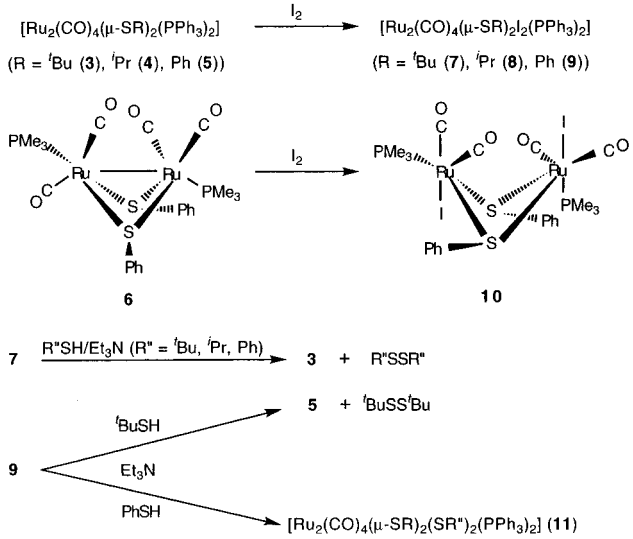

acetone-d_6 at 300 and 220 K. The long distance with d(Ru···Ru) = 3.743 Å between two Ru atoms indicates no Ru−Ru single bond in **10** and probably also in **7**−**9**. The two iodides are trans to each other, reflecting a trans addition of diiodine to **6** and probably also to **3**−**5**. If the resulting structure **7**−**9** has two trans iodide atoms with each at one Ru atom, the observed $^{31}P\{^1H\}$ NMR singlet at δ 44.58 for **7**, 46.65 for **8**, and 50.97 for **9** in acetone-d_6 at 300 and 220 K may suggest a very facile process, probably involving conversion of two terminal into bridging iodides concomitantly with opening two bridging into terminal thiolato groups while not permitting rotation of two carbonyls and one phosphine attached to each Ru atom along a pseudo-C_3 axis (Scheme 4), resulting in two equivalent and inequivalent phosphine atoms for **7**−**9** and **10**, respectively, at the NMR time scale. The evidence of the three-band ν_{CO} pattern and the one $^{31}P\{^1H\}$ NMR singlet described for

Scheme 4

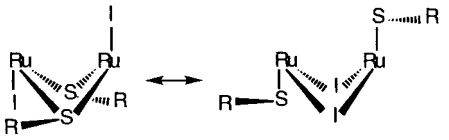

Scheme 5

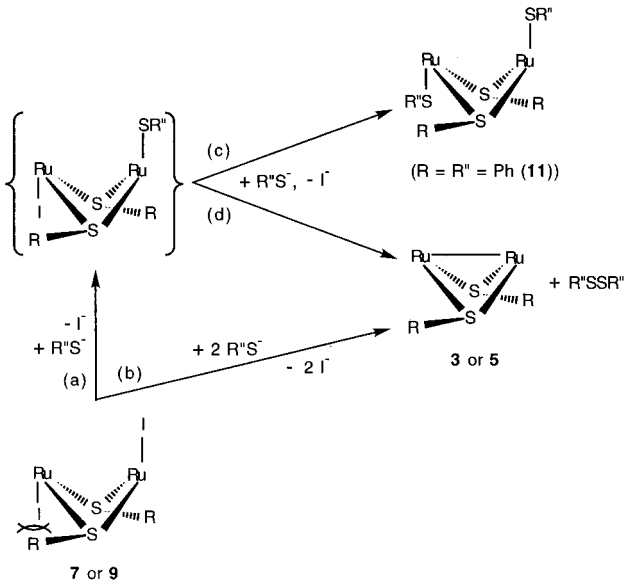

7−**9** and that of one ^{1}H NMR singlet at δ 0.76 for the two ^{t}Bu groups in **7**, one doublet at 0.95 and one heptet at 2.99 for two ^{i}Pr groups in **8**, and one ^{31}C NMR doublet at 192.5 with $J_{P,C}$ = 11.0 Hz[13] for the four carbonyl groups in **9** suggest that **7**−**9** should adopt probably the syn form rather than the anti form.

The reported reaction chemistry of $[Fe_2(CO)_4(\mu\text{-}SR)_2(PPh_3)_2]$ (R = Et, Ph) with X_2 (X = Cl, Br, I) is quite rich, producing either $[Fe_2(CO)_4(\mu\text{-}SR)_2(PPh_3)_2I]I_3$ or $[Fe_3(CO)_4(\mu\text{-}SR)_2(PPh_3)_2X_4]X$ with no Fe−Fe metal bond.[4b] However, decarbonylation occurs quite readily for iodination of **7**-**9**, resulting in intractable products, apparently without carbonyl groups attached to the metal center on the basis of the IR spectra obtained. Reactions of **7**−**9** with nucleophiles such as thiolate anions were then carried out. The reaction results between complexes **7** and **9** and the anions via R″SH/Et_3N (R″ = ^{t}Bu, ^{i}Pr, Ph) appear somewhat unexpectedly to have two reaction pathways. Among the five reactions studied, only the one between **9** and PhS^- gave the expected substitution product, $[Ru_2(CO)_4(\mu\text{-}SPh)_2(SPh)_2(PPh_3)_2]$ (**11**). Other reactions regenerated reductively **3** and **5** with the apparently external R″S anions being oxidized into R″SSR″ in high yield (Scheme 3). Disulfide formation was previously reported for the internally ligated thiolato groups of $[Fe_2(CO)_6(\mu\text{-}SR)_2]$ but under oxidation conditions with O_2,[4j] different from our examples. Under similar reaction conditions with excess R″SH/Et_3N relative to the complex (e.g., 1 mL of R″SH, 2 mL of Et_3N, and ca. 0.30 mmol of the complex), we found that the time required for a complete redox reaction is ca. 2 h, much *longer* than that of 0.5 h needed for a complete substitution reaction. Further, on the basis of the IR spectra measured sequentially for the longer redox reaction, no intermediate compounds were observed with typical IR spectra recorded in an overlaid mode for the reaction between **7** and PhSH/Et_3N in CH_2Cl_2. These facts led us to propose a mechanism favoring substitution (route a) rather than a redox process (route b) for the first step of the reaction.[15] It probably involves the replacement of one iodide at the less sterically congested site (cf. Scheme 5) with one thiolate anion to form the intermediate $[Ru_2(CO)_4(\mu\text{-}SR)_2(SR'')I(PR'_3)_2]$. For PhS^-, the steric hindrance of this intermediate with R = R′ = R″ = Ph is not large, enabling a further replacement reaction (route c) to give **11**. However, when the hindrance of the intermediate with one of the other combinations of R, R′, and R″ (i.e., R = R′ = Ph, R″ = ^{t}Bu; or R = Ph, R′ = ^{t}Bu, R″ = Ph, ^{i}Pr, or ^{t}Bu) is too high to allow a second replacement reaction, a redox reaction (route d) occurs with regeneration of complexes **3** and **5** and R″SSR″.

Like **9**, **11** displays one ^{31}P{^{1}H} NMR singlet for the two PPh_3 ligands in this compound dissolved in CH_2Cl_2 at 300 or 220 K, suggesting a similar facile process involving conversion of two terminal into bridging thiolato groups concomitantly with opening two bridging into terminal thiolato groups (cf. Scheme 4) to make two phosphine atoms equivalent at the NMR time scale. However, the two structures are different, with a syn form for **9** and an anti form for **11**, based on the two observed ^{13}C NMR doublets at δ197.2 (J = 8.3 Hz)[13] and 197.5 (J = 9.7 Hz)[13] for the four carbonyls in this compound dissolved in $CDCl_3$. Apparently, it is rather difficult to predict the structure preference for any diruthenium compounds with two thiolato bridges prior to examining the characterization data. The two thiolato bridges in a dinuclear system may adopt a syn form like **3** and **7**−**10** or an anti form like **6** and **11**, or they may involve an equilibrium mixture of syn and anti forms with the syn form favored for **4** and the anti form for **5** in solution. This nonspecific feature is probably more associated with steric effects than electronic effects, and the one or two forms adopted may represent nonbonded interactions of low, if not the least, repulsiveness.

Conclusion

Our investigation into diruthenium carbonyl phosphine complexes containing two μ-thiolato linkages resulted in the facile synthesis of **3**−**6** from **1** and **2** in satisfactory yield (Scheme 1). Electrophilic additions of **3**−**6** with I_2 produce diiodide adducts **7**−**10**. Further reactions of **7** and **9** with thiolate anions give either expected nucleophilic substitution products such as **11** or unexpected reductive-dehalogenation to regenerate complexes **3** and **5**, respectively, with the apparently external anions being oxidized into alkyl or aryl disulfides (Scheme 3). Various spectral data and five X-ray crystal structures (Figures 1−5) help to establish that the two thiolato bridges in **3**−**11** may adopt a syn form or an anti form, or they may involve an equilibrium mixture of both forms with one form or the other favored in solution. An unprecedented structure type with the two thiolato bridges located cis to one of two phosphine ligands in the compounds but trans to the other was

(13) The coupling constant is compatible with the reported values.[14]

(14) Gill, D. F.; Mann, B. E.; Shaw, B. L. *J. Chem. Soc., Dalton Trans.* **1973**, 311.

(15) Astruc, D., Ed. *Electron Transfer and Radical Processes in Transition-Metal Chemistry*; VCH: New York, 1995.

observed in **6** (Figure 4) and retained in the iodination product **10** (Figure 5), in spite of the anti geometry in **6** being changed into syn in **10**.

Acknowledgment. Financial support for this work by the National Science Council of Republic of China (Contract NSC87-2113-M006-007) and skillful assistance by Ms. Fang-Chung Chou are gratefully acknowledged.

Supporting Information Available: Tables of non-hydrogen atomic coordinates and equivalent isotropic displacement coefficients, complete bond lengths and angles, anisotropic displacement coefficients, and hydrogen coordinates for **3**, **4A**, **5B**, **6**, and **10** (30 pages). Ordering information is given on any current masthead page.

OM9710024